High-resolution electron spectroscopy of a strongly correlated system: Atomic barium

G. Snell,[1,2] M. Martins,[3] E. Kukk,[1,2,*] W. T. Cheng,[1,4] and N. Berrah[1]
[1]*Department of Physics, Western Michigan University, Kalamazoo, Michigan 49008-5151*
[2]*Lawrence Berkeley National Laboratory, University of California, Berkeley, California 94720*
[3]*Institut für Experimentalphysik, Freie Universität Berlin, D-14195 Berlin, Germany*
[4]*Department of Physics, National Central University, Chung-Li, Taiwan, 32054, Republic of China*
(Received 6 September 2000; published 11 May 2001)

High-resolution $4d$ and $5p$ photoelectron spectra of free barium atoms were measured using narrow-bandwidth synchrotron radiation of 131.2 eV photon energy. These measurements were necessary to disentangle the complex structure of the electron spectra. We also performed a Hartree-Fock calculation with relativistic corrections. A very good agreement between theory and experiment was found, which allowed the assignment of all but the weakest lines, in addition to pointing out the significant contribution of configuration interaction and shake processes.

DOI: 10.1103/PhysRevA.63.062715 PACS number(s): 32.80.Hd, 32.80.Fb

I. INTRODUCTION

Inner-shell photoionization studies in alkaline-earth metals performed in the 1970s and early 1980s have been very beneficial in understanding the electronic structure of free atoms [1]. Barium in particular has been studied by photoabsorption [2,3] and electron-impact [1,4] measurements. More recently, electron-ion coincidence spectroscopy on atomic Ba in the excitation range of $4d$ giant resonance was carried out by Baier *et al.* [5]. Barium is still a very interesting case to study, especially the $5p$ and $4d$ excitations, because the near degeneracy of the $6s$ and $5d$ subshells leads to very complex photoionization spectra, which are very rich in strong configuration mixing [6,7] and shakeup satellites [8]. Indeed, early measurements [1,4] and a fully relativistic analysis of the $5p$ excitation in Ba by Rose *et al.* [7], revealed an extremely complex structure. Photoelectron work by Bizau *et al.* [8] and others [9–12] also showed complexity in the spectra following $5p$ and $4d$ excitation. However, detailed experimental studies could not be carried out due to limitations in the available synchrotron radiation sources and electron spectrometers. With the advent of third generation light sources, allowing higher photon intensity and resolution, coupled with high-resolution electron spectrometers, detailed measurements can be carried out and compared with the most recent *ab initio* calculations. The present paper reports high-resolution measurements and calculations of the Ba $5p$ and $4d$ photoionization processes. A comparison with previous calculations [11–16] and measurements [4,8,9,11] is also presented.

II. EXPERIMENT

The experiment was performed at the Atomic and Molecular beamline 10.0.1 of the Advanced Light Source synchrotron radiation facility at Lawrence Berkeley National Laboratory. The radiation from a 4.5-m-long 10-cm period undulator was monochromatized by a spherical grating monochromator. A photon bandwidth of 40–50 meV was used with the 925 lines/mm grating at 131.2 eV photon energy. The electron spectra were measured using an end station designed for gas-phase angle-resolved studies, which is based on a Scienta SES-200 hemispherical analyzer [17]. The present measurements were all performed at an emission angle of 54.7° with respect to the electric-field vector, in a plane perpendicular to the propagation direction of the linearly polarized photon beam. The analyzer was operated at a constant pass energy of 40 eV, with an electron energy resolution of 40–50 meV. The kinetic-energy scale of the spectrometer was calibrated by the Xe NOO Auger lines [18], and the photon energy was determined using the binding energy of the Xe $4d$ photolines.

A resistively heated metal vapor oven was used to generate an effusive beam of Ba atoms. To increase the length of the interaction region, the nozzle of the stainless-steel crucible contained eight channels (0.8 mm diameter, 5 mm long) in a line, aligned parallel to the photon beam direction. A 1.5-mm-thick μ-metal disk with a slit for the atomic beam was placed between the crucible and the interaction region to shield the magnetic field of the heater, the crucible, and other parts of the oven from the interaction region. On the other side of the interaction region, opposite to the crucible, a water-cooled copper disk was mounted to collect and condense the metal vapor. The contact potential of the accumulating Ba on this disk caused a continuously changing field in the interaction region. To keep the highest possible electron energy resolution over a long period of time, the electron spectra were collected by one sweep at a time and added up later taking into account small shifts of a few meV. The operating temperature of the oven was in the range of 540–590 °C, at which the Ba vapor pressure inside the crucible was in the range of 1.5–5.0 mtorr [19].

III. THEORY

Theoretical description of the Ba photoionization process has been a challenge for a long time, due to its strong correlation effects. The $4d \rightarrow (4,\epsilon)f$ photoabsorption is dominated by a strong shape resonance. Photoionization cross sections in Ba were described successfully by advanced many-body theories such as the random-phase approximation with exchange [20] and many-body perturbation theory (MBPT)

*Present address: Department of Physical Sciences, University of Oulu, P.O. Box 3000, FIN-90014 Oulu, Finland.

TABLE I. Basis set used for the calculation of the photoemission spectra. Configuration interaction (CI) is included in the ground state (GSCI) and the final ionic state (FISCI).

Configuration
Ground state
$6s^2$, $6p^2$, $5d^2$, $4f^2$
Final ionic state after $4d$ excitation
$4d^9 6s^2$, $4d^9 6p^2$, $4d^9 5d^2$, $4d^9 4f^2$, $4d^9 6s7s$, $4d^9 5d7s$, $4d^9 6p4f$, $4d^9 6s5d$, $4d^9 6s6d$, $4d^9 6p7p$, $4d^9 6p5f$, $4d^9 6p6f$
Final ionic state after $5p$ excitation
$5p^5 6s^2$, $5p^5 6s5d$, $5p^5 5d^2$, $5p^5 6p^2$, $5p^5 4f^2$, $5p^5 6s7s$, $5p^5 6s6d$, $5p^5 6p4f$, $5p^5 5d7s$, $5p^5 5d6d$

[13,15]. Strong correlation effects can also be observed in $4d$ photoemission spectra [8–12]. These effects were studied theoretically in Refs. [15] and [16] using MBPT and Hartree-Fock (HF) calculations, respectively. Matila and Aksela have already shown [16] that a HF calculation can give a good description of Ba electron spectra, if electron correlation is taken into account. In the present paper we calculated HF wave functions with relativistic and correlation corrections. Dipole matrix elements were calculated in an intermediate coupling scheme with the standard Slater-Condon superposition of configuration method using the Cowan code [21]. In HF calculations energy-level splittings resulting from electron-electron Coulomb interactions are too large, because LS-term-dependent electron correlations are neglected (see Ref. [21] (see Ref. [21], Chap. 16-2). Therefore, all Coulomb integrals F^k, G^k, and R^k have been scaled by 85%, which is reasonable for HF calculations of neutral atoms and singly charged ions. It is known from photoabsorption calculations [15] and the detailed analysis in Ref. [16] that very strong configuration interaction (CI) has to be taken into account in the case of Ba. Therefore, in the ground-state [Xe] $6s^2$ ($^1S_0$), ground- state configuration interaction (GSCI) has been included with the configurations $6p^2$, $5d^2$, and $4f^2$.

As in the ground state, strong correlations also had to be included in the final state of the photoionization process. This was done in a first approximation by final ionic state configuration interaction (FISCI) between the configurations $4d^9 6s^2$, $4d^9 6s5d$, $4d^9 6p^2$, $4d^9 5d^2$, and $4d^9 4f^2$ for the $4d$ excitation. However, as reported by Matila and Aksela, several more configurations have to be included in order to obtain a good agreement between the experiment and theory [16]. The same is also valid for the final state of the $5p$ photoexcitation. The configurations used in our calculations are given in Table I. Our calculations show that including even more configurations does not improve the results further.

Another main contribution to the $4d$ photoemission are satellites of the types $4d^{-1}6s7s$, $4d^{-1}6s6p$, and $4d^{-1}6s4f$, which appear in the same energy range as the main lines and the CI satellites, whereas for the $5p$ excitation they are more separated [11]. The $4d^{-1}6s7s$ satellites can be populated by FISCI, due to the same parity as the final states, but the $6s6p$ and $6s4f$ satellites can only be excited by a conjugate shakeup process. Shakeup satellites arise in the sudden approximation, where the photoionization causes a sudden change in the Coulomb attraction. This excitation channel is also possible for $6s7s$ satellites. To estimate the intensities of the shake satellites, several overlap integrals have been calculated. Following the shake theory [22] the intensity of the $6sns$ shake satellite is given by

$$|\langle 6s|ns\rangle\langle 6s|6s'\rangle\langle 4d|e\vec{r}|\epsilon f\rangle|^2,$$

whereas the main line is described by

$$|\langle 6s|6s'\rangle^2\langle 4d|e\vec{r}|\epsilon f\rangle|^2.$$

The conjugate shake process can be estimated by

$$|\langle 6s|6s'\rangle\langle 6s|e\vec{r}|np\rangle\langle 4d|\epsilon d\rangle|^2.$$

Here $6s$ and $6s'$ are the $6s$ wave functions in the ground state and the intermediate core excited state, respectively. This method fails in the case of the $6s4f$ satellite, since $\Delta l = 3$ and the dipole matrix element $\langle 6s|e\vec{r}|4f\rangle$ will always be zero.

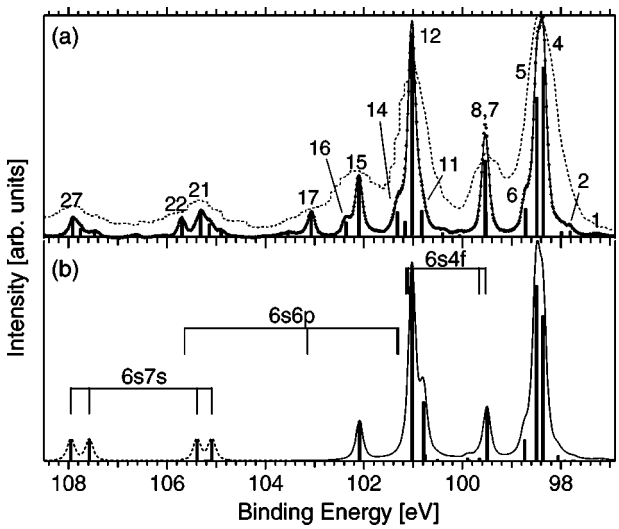

FIG. 1. Barium $4d$ photoelectron spectra. (a) Data recorded at 131.2-eV photon energy, with a photon bandwidth of 50 meV and a spectrometer resolution of 50 meV. A linear background was subtracted from the spectrum. The solid line represents a fit with Voigt profiles. The dashed line is from Ref. [8]. (b) Calculated spectrum using the relativistic Hartree-Fock method (solid line) and overlap integrals (dashed line). The vertical bars represent the fitted (a) and calculated (b) lines. The assignments are given in Table II.

IV. RESULTS AND DISCUSSION

A. $4d$ photoionization

Our experimental and calculated spectra are shown in Fig. 1 together with previous data of Bizau *et al.* [8]. The measurements were performed with a photon bandwidth of 50 meV and a spectrometer resolution of 50 meV. In the strongest line (12) 66 500 counts were collected during approximately 100 min of acquisition time. The spectrum was fitted

TABLE II. Binding energies, relative intensities, and assignments of the Ba^+ $4d^{-1}$ ionic states.

Line	Binding energy (eV)				Intensity		Assignment of the $4d^9$ states		
	This work		Ref. [9]	Ref. [8]	This work		Ref. [9]	Ref. [11]	This work
	Expt.	Theory	Expt.	Expt.	Expt.	Theory			
1	97.25(1)				1.4				
2	97.82(1)				3.1				
3	97.99(2)	98.06			2.8	2.8			$5d^2\,{}^2F_{5/2}$
4	98.360(1)	98.36	98.4(2)	98.41(6)	83.7	74.3	$6s^2, J=5/2$	$5d^2, J=5/2$	$5d^2\,{}^2F_{5/2}$
5	98.489(1)	98.50			68.7	89.7		$6s^2, J=5/2$	$6s^2\,D_{5/2}$
6	98.716(2)	98.74			14.3	10.9			$5d^2\,{}^2D_{5/2}$
7	99.535(1)	99.50			37.7	26.8		$5d^2, 6s5d, J=5/2$	$5d^2\,{}^2D_{5/2}$
		99.53 [a]	99.5(2)	99.50(10)			$6s4f, J=5/2$		$(^1D)6s4f\,{}^2D_{3/2}$
8	99.535(1)				12.4			$5d^2, J=5/2$	
		99.66 [a]							$(^3D)6s4f\,{}^2D_{5/2}$
9	100.06(2)				1.4				
10	100.41(2)				2.3				$5d6p$ [b]
11	100.824(3)	100.79			13.0	30.1		$6s^2, J=3/2$	$6s4d\,{}^2D_{3/2}$
12	101.023(1)	101.02			100.0	100.0		$6s5d, J=3/2$	$6s^2\,{}^2D_{3/2}$
		101.10 [a]							$(^1D)6s4f\,{}^2D_{5/2}$
13	101.169(5)		101.0(2)	101.02(6)	7.9		$6s^2, J=3/2$		
		101.14 [a]							$(^3D)6s4f\,{}^2D_{3/2}$
		101.18 [a]							$(^1D)6s6p\,{}^2D_{3/2}$
14	101.324(2)				12.7				
		101.20 [a]							$(^1D)6s6p\,{}^2D_{5/2}$
15	102.103(1)	102.09			29.2	20.3			$6p4f\,{}^4F_{5/2}$
			102.0(2)	102.20(10)			$6s4f, J=3/2$	$5d^2, J=3/2$	
16	102.359(3)				7.5				$5d4f$ [b]
17	103.076(2)	103.02 [a]	103.1(2)	103.10(15)	11.9		$6s6p, J=5/2$	$6s7s, J=5/2$	$(^3D)6s6p\,{}^2D_{5/2}$
18	103.55(1)				2.8			$6s7s, J=5/2$	
19	104.904(5)				2.6				
20	105.137(3)	105.09 [a]	105.3(2)		6.7	11 [c]	$6s7s, J=5/2$	$6p^2, 4f^2, J=5/2$	$(^1D)6s7s\,{}^2D_{3/2}$
21	105.320(2)	105.39 [a]		105.25(25)	12.2	11 [c]		$rf^2, J=5/2$	$(^3D)6s7s\,{}^2D_{5/2}$
22	105.698(2)	105.52 [a]	106.0(2)		8.6		$6s6p, J=3/2$	$6s7s, J=3/2$	$(^3D)6s6p\,{}^2D_{3/2}$
23	106.12(2)				0.4				
24	106.64(1)				0.8			$6s7s, J=3/2$	
25	107.475(5)				2.8				
		107.58 [a]				11 [c]		$6p^2, 4f^2, J=3/2$	$(^1D)6s7s\,{}^2D_{5/2}$ [d]
26	107.761(4)		107.7(2)	107.70(15)	4.2		$6s7s, J=3/2$		
27	107.912(2)	107.95 [a]			8.8	11 [c]		$4f^2, J=3/2$	$(^3D)6s7s\,{}^2D_{3/2}$

[a] Binding energy determined from an electronic structure calculation.

[b] Tentative assignment.

[c] Intensity estimated from overlap integrals.

[d] A clear assignment to line 25 or 26 is not possible.

with a set of Voigt profiles, where the Lorentzian and Gaussian widths (with the exception of lines 18, 23, and 24) were kept the same for all lines [23]. A natural linewidth of 113(10) meV and a Gaussian broadening of 109(10) meV was obtained from the fit. The uncertainties of the fit parameters were determined by using the Monte Carlo method on simulated data sets [24]. The fitted positions and intensities of the peaks are indicated as vertical lines in the top panel of Fig. 1, and are listed in Table II. Whereas the relative positions within the spectrum can be determined accurately, an absolute calibration of the kinetic energy scale is difficult due to the continuously changing contact potential during the measurement. We estimate this calibration uncertainty to be on the order of 10–20 meV. The calculated lines are shown as vertical lines in the lower panel of Fig. 1, and are also listed in Table II. For better comparison the theoretical data were convoluted with a 109-meV Gaussian and a 113-meV Lorentzian to match the experimental resolution and lifetime broadening, respectively.

The position and intensity of the calculated spectrum were matched to the measurement using line 12 by shifting the theoretical spectrum by 0.1 eV. For the main lines in the region of 98–102 eV binding energy, an excellent agreement is found for the line positions. The intensity distribution is

TABLE III. Intensities of the Ba $4d$ shake satellites relative to the $6s^2$ main lines for $E_{kin}=26$ eV. The theoretical values have been evaluated by calculating simple overlap integrals as described in the text.

Shake satellite	Intensity	
	Theory	Expt.
$6s^2$	1	1
$6s7s$	0.11	0.1
$6s6p$	0.003	0.1

also given rather well by the calculation, although some intensity is missing at 99.5-eV binding-energy (lines 7 and 8), and the ratio of lines 4 and 5 is reversed. The satellite structure in this region is almost completely due to configuration interaction, which is taken into account in the present calculation using the basis sets given in Table I. These lines can be assigned to the $4d^96s^2$, $4d^95d^2$, $4d^96s5d$, and $4d^96p4f$ states (cf. Table II).

Above 102-eV binding energy, considerable intensity is missing in the calculated spectrum. It is known from previous works [8,9,11] that the satellite lines above 102 eV are mostly due to the $4d^96s7s$ shakeup process and $4d^96s4f$ and $4d^96s6p$ conjugate shakeup processes. The missing intensity is expected for conjugate shake satellites because they cannot be taken into account in the present calculation. The normal shake satellites $4d^96s7s$ have been included via CI, but their estimated intensity is too low. To identify the experimentally observed lines, we determined the binding energy of the shake satellites from an electronic structure calculation. In Fig. 1(b) the positions of these satellites are marked by vertical bars. For simplification only the ^2D states are shown. The positions are in very good agreement with observed satellite lines. For the configuration $6s7s$ mixing with the $5d7s$, which are located at lower binding energies, is most important. Neglecting this effect will result in binding energies that are about 0.3 eV too low. The influence of the comparable configurations $5d6p$ and $5d4f$ on the conjugate shake satellites $6s6p$ and $6s4f$ is much weaker. Nevertheless, the intensities of the satellites cannot be evaluated in this simple CI picture. This leads to the conclusion that the $4d^96s7s$ satellite lines are mainly populated by shake processes and not by final ionic state configuration interaction, which is the main process for the $4d^95d^2$, $4d^96s5d$, and $4d^96p4f$ states. To estimate the intensities for the shake satellites, we have calculated several overlap integrals as described above. These intensities are given in Table III together with the experimental values. A very good agreement is achieved for the normal shakeup intensities calculated in this approximation with the experimental data, and also with the values given in Ref. [16]. However, this simple approximation fails for the conjugate shake process. This also explains the missing intensities in the theoretical spectrum at 99.5 and 101.2-eV binding energies. Thus lines 7 and 13 can be attributed to the $6s4f$ conjugate shakeup satellites.

A similar problem of underestimating the conjugate shakeup intensities based on overlap integrals of the radial HF wave functions was encountered in the study of Li $1s$ photoionization [25,26]. Electron-electron interaction processes beyond the reach of the self-consistent-field approach can also create conjugate shakeup final states, and thus greatly enhance the intensities of these lines. One such mechanism, referred to as ''direct knock-out'' by Amusia [27], describes inelastic scattering of the outgoing photoelectron on the bound electrons of the atom, exciting or ionizing them, and involving redistribution of the electron angular momenta. In the present case, $6s\rightarrow 6p$ excitations can be due to such scattering processes. The importance of direct knock-out in $4d$ photoionization is also emphasized by the fact that the cross-section calculations are in a better agreement with experiment if these processes are taken into account [27,28].

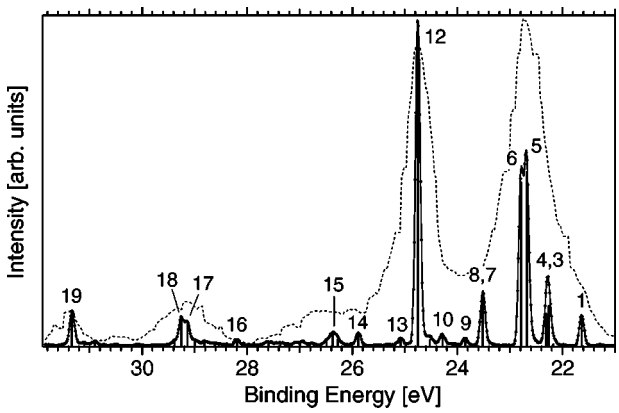

FIG. 2. Barium $5p$ photoelectron spectrum recorded at 131.2-eV photon energy with a photon bandwidth of 50 meV and a spectrometer resolution of 50 meV. The vertical lines represent the fitted peaks. The solid line represents a fit with Voigt profiles. The dashed line is from Ref. [8]. The assignments are given in Table IV.

B. $5p$ photoionization

Measured and calculated Ba $5p$ spectra are shown in Figs. 2 and 3. In Fig. 2 experimental data of Bizau et al. [8] is also shown. According to a one-electron model, only two Ba II levels, $5p^56s^2$ ($^2P_{1/2}$) and $5p^56s^2$ ($^2P_{3/2}$), should be observed, yet the electron impact measurements [1,4] as well as our photoelectron spectra reveal a much richer structure. This is due to CI, which is considerable in the singly ionized states, in addition to shakeup processes [7,11].

In the low-resolution spectrum (Fig. 2), 18 500 counts were collected in the strongest line (12) during 200 min of acquisition time at an oven temperature of 550 °C. In the high-resolution spectrum [Fig. 3(a)], 12 200 counts were accumulated in the same line during 110 min at an oven temperature of 590 °C. The spectra were fitted with a set of Voigt profiles, where the Lorentzian and Gaussian widths for most lines were kept the same and a linear background was used [23]. The positions and intensities of the lines are indicated as vertical bars in Figs. 2 and 3 and are listed in Tables IV and V. Some weak and broad features between lines 15 and 19 were fitted by broad Gaussian curves. Furthermore, an asymmetric line shape was used. The distortion of the lines was probably caused by a weak magnetic field emerging from the oven. The analysis yielded a Lorentzian line-

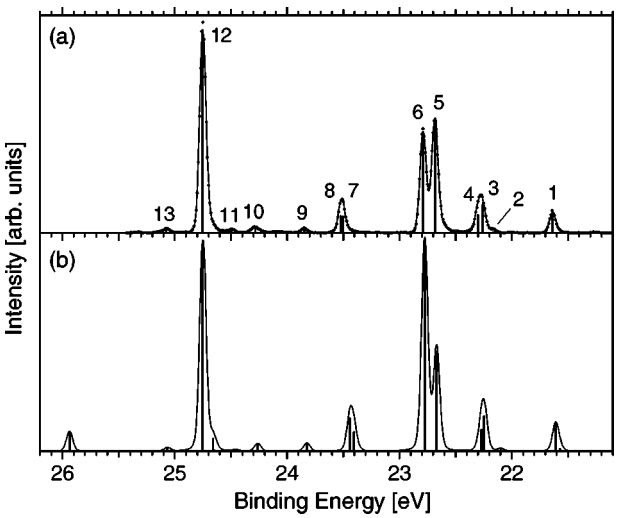

FIG. 3. (a) Barium $5p$ photoelectron spectrum recorded at 131.2 eV photon energy with a photon bandwidth of 40 meV and a spectrometer resolution of 40 meV. The solid line represents a fit with Voigt profiles. (b) Calculated spectrum using the relativistic Hartree-Fock method. The vertical bars represent the fitted (a) and calculated (b) lines. The assignments are given in Table IV.

width of 13 meV in both spectra, and Gaussian broadenings of 96 and 59 meV for the low- and high-resolution spectra, respectively.

The main photoelectron lines, labeled 5, 6, and 12 in the figure, are accompanied by correlation and/or shakeup satellites. In the case of the $5p$ excitation, the satellite structure is expected to arise mostly from CI between the $6s^2$, $5d6s$, and $5d^2$ configurations in the presence of a $5p$ hole, and from the $6s \rightarrow 7s$ shakeup process [4,6,7]. In our calculation of the $5p$ photoemission, correlation effects in the ground state (GSCI) and final state (FISCI) are included by using the basis set of Table I. The theoretical spectrum has been shifted by 88 meV to match the experiment at line number

TABLE V. Relative intensities of the Ba^+ $5p^{-1}$ ionic states.

Line	Intensity			
	This work		Ref. [11]	
	Expt.	Theory	Expt.	Theory
19	10.5		12	7
18	8.5		5	9
17	6.8		22	12
16	1.8	6		21
15	3.9	1.6	10	7
14	4.0	9.4	6	6
13	2.1	1.6		
12	100.0	100.0	100	100
11	1.0	0.6		4
10	3.1	3.6		3
9	2.1	3.9	3	1
8	8.7	16.3	23	17
7	8.5	9.5		
6	49.8	99.8	73	67
5	55.3	48.7	65	86
4	9.2	10.7		3
3	14.2	17.3	18	20
2	0.9	1.2		
1	10.2	13.3	12	31

TABLE IV. Binding energies, and assignments of the Ba^+ $5p^{-1}$ ionic states.

Line	Binding energy (eV)					Assignment of the $5p^5$ states			LS
	This work		Ref. [8]	Ref. [4]	Ref. [16]	This work	Ref. [11]	Ref. [7]	Purity
	Expt.	Theory	Expt.	Expt.	Theory				
19	31.337(3)		31.3(1)	31.336(3)			$6p^2$		
18	29.254(4)		29.2(1)	29.158(3)			$6s7s$		
17	29.142(4)		,,				$6p^2$		
16	28.195(5)						$6s7s$		
15	26.374(6)	26.52	26.3(2)	26.393(1)	26.53	$5d^2\,(^3P)\,^2P_{1/2}$	$5d^2$		0.321
14	25.889(4)	25.94				$5d^2\,(^1S)\,^2P_{1/2}$	$5d^2$		0.390
13	25.083(7)	25.07				$5d^2\,(^3D)\,^2D_{3/2}$	$5d^2$		0.157
12	24.755(1)	24.76	24.75(2)	24.755(1)	24.88	$6s^2\,(^1S)\,^2P_{1/2}$	$6s^2$	$6s^2$	0.753
11	24.499(5)	24.46				$5d^2\,(^1D)\,^2P_{3/2}$	$5d^2$		0.616
10	24.287(4)	24.27	24.20(3)	24.123(1)		$5d^2\,(^3P)\,^4S_{3/2}$	$5d6s$		0.345
9	23.853(4)	23.83	,,			$6s5d\,(^3D)\,^4D_{3/2}$	$5d6s$		0.519
8	23.527(5)	23.45	23.51(3)	23.516(1)	23.72	$5d^2\,(^1D)\,^2D_{3/2}$	$5d^2$	$5d6s$	0.143
7	23.508(5)	23.41				$5d^2\,(^3P)\,^2D_{3/2}$			0.410
6	22.793(2)	22.78	22.72(2)	22.794(1)	23.05	$6s^2\,(^1S)\,^2P_{3/2}$	$5d6s$	$5d^2$	0.409
5	22.687(2)	22.67	,,	22.688(1)	22.89	$5d^2\,(^1S)\,^2P_{3/2}$	$5d^2$	$6s^2$	0.180
4	22.306(4)	22.28	22.27(3)			$6s5d\,(^3F)\,^4F_{3/2}$	$5d6s$		0.306
3	22.266(2)	22.25	,,	22.229(1)	22.42	$5d^2\,(^3F)\,^4F_{3/2}$	$5d^2$	$5d^2$	0.228
2	22.171(16)	22.10				$5d^2\,(^3P)\,^4P_{3/2}$			0.602
1	21.639(4)	21.61	21.60(4)	21.64(1)	21.7	$5d^2\,(^3P)\,^2P_{3/2}$	$5d^2$	$5d^2$	0.287

12. Shake processes are not included. According to Mäntykenttä *et al.* [11], the classification of the satellites as CI or shakeup is related to the calculation method since the probabilities in the first case are obtained from the mixing coefficients and in the second from the overlap integrals. In their calculations, configuration interaction in the ground state of Ba is so weak that it is neglected. Also, in order to determine the strength of CI in the case of the $5p$ hole, the MCDF calculation included the $5p^5 6s^2$, $5p^5 5d 6s$, $5p^5 5d^2$, $5p^5 6p^2$, $5p^5 4f^2$, and $5p^5 6s 7s$ configurations with total angular momenta $J=1/2$ and 3/2.

In Table IV, we report our experimental and theoretical binding energies of 19 lines corresponding to the main and CI satellites lines. Our results are compared with previous measurements [4,8,11], and the agreement among the listed values is excellent. There is also a very good agreement between the experimental and theoretical spectra. Even the very small satellite 2 is well described by the calculation. In Table IV our data are also compared with the recent configuration interaction Hartree-Fock calculation of Matila and Aksela [16]. This calculation also included a mixing of configurations with the outermost valence electrons ($nl = 6s, 5d, 6p, 4f$), and gave similar results.

Previous assignments of Refs. [7,11] are compared with ours in Table IV. All assignments agree in the case of lines 1, 3, and 12, and they all disagree in the case of line 6. However, Ref. [7] disagrees with Ref. [11] and our assignment in the case of lines 5 and 8. This problem in assigning the states to configurations arises almost certainly from the strong intermediate coupling of the $5p$ final states. This leads to eigenvectors, where different configurations can have nearly the same contribution to the state. This can also be seen from the purity of the states shown in Table IV, which are typically only around 30% in LS coupling. In jj coupling we obtained a very similar result. Therefore, the $5p$ spectrum of atomic barium is an example of a strongly mixed system, where only the angular quantum number J of the final ionic state is a good quantum number and even the configuration due to strong correlations is only a rough description of the state. An exception is line 12, which has a purity of 75% in LS coupling. Therefore, the chosen set of configurations can have a large influence on the dominating part of the wave function, resulting in discrepancies between the three assignments.

Table V reports some measured and calculated relative intensities of the observed main and satellite lines. The comparison between our results and those of Mäntykenttä *et al.* shows that in Ref. [11] both the experimental and calculated values are systematically higher than our results. However, according to Ref. [11], the relative line intensities are not necessarily accurate close to threshold in the sudden approximation, and this may be the explanation for the discrepancy. Our calculations also tend to be higher than our measurements, but not as high as those of Ref. [11].

V. SUMMARY

We have performed high-resolution measurements of the Ba $4d$ and $5p$ photoelectron spectra using monochromatized synchrotron radiation of 131.2 eV photon energy. High-resolution measurements were necessary to disentangle the rich line structure of the electron spectra, which is caused by configuration interaction and shake processes. To interpret the experimental results, a Hartree-Fock calculation with relativistic corrections was carried out. A very good agreement between theory and experiment was found, which allowed the assignment of all but the weakest lines of the $4d$ and $5p$ photoemission spectra.

In the case of the $4d$ photoionization process, the satellite structure in the vicinity of the main lines is mostly due to configuration interaction, it is populated by the $4d^9 6s^2$, $4d^9 5d^2$, $4d^9 6s 5d$, and $4d^9 6p 4f$ states. A small contribution ($\approx 10\%$) from the $4d^9 6s 4f$ conjugate shakeup process is also present. The satellites at higher binding energies are mostly due to the $4d^9 6s 7s$ shakeup and $4d^9 6s 6p$ conjugate shakeup excitations.

In the case of the $5p$ photoionization process, CI in the final ionic states is found to be the main factor. Specifically, the complex satellite structure arises from CI between the $5p^5 6s^2$, $5p^5 5d^2$, and $5p^5 6s 5d$ configurations, with a small contribution from $6s \rightarrow 7s$ shakeup processes.

It is probably not possible to obtain more information about the studied processes just by increasing the experimental resolution further. The $4d$ spectra are limited by lifetime broadening and in the $5p$ spectra most of the lines are already separated. Angle- and spin-resolved measurements might shed more light on the unexplained details.

ACKNOWLEDGMENTS

We would like to thank the ALS staff, especially Dr. J. D. Bozek, for providing excellent working conditions. This work was supported by the Department of Energy, Office of Science, Basic Energy Sciences, Chemical Sciences Division. The Advanced Light Source is supported by the Department of Energy, Materials Sciences Division.

[1] D. Rassi and K. J. Ross, J. Phys. B **13**, 4683 (1980), and references therein.

[2] G. Wendin, Phys. Lett. **51A**, 291 (1975).

[3] D. L. Ederer, T. B. Lucatorto, E. B. Saloman, R. P. Madden, and J. Sugar, J. Phys. B **8**, L21 (1975).

[4] W. Mehlhorn, B. Breuckmann, and D. Hausamann, Phys. Scr. **16**, 177 (1977).

[5] S. Baier, G. Gottschalk, T. Kerkau, T. Luhmann, M. Martins, M. Richter, G. Snell, and P. Zimmermann, Phys. Rev. Lett. **72**, 2847 (1994).

[6] J. P. Connerade, M. W. D. Mansfield, G. H. Newsom, D. H. Tracy, M. A. Baig, and K. Thimm, Philos. Trans. R. Soc. London, Ser. A **290**, 327 (1979).

[7] S. J. Rose, I. P. Grant, and J. P. Connerade, Philos. Trans. R.

Soc. London, Ser. A **296**, 527 (1980).
[8] J. M. Bizau, D. Cubaynes, P. Gerard, and F. J. Wuilleumier, Phys. Rev. A **40**, 3002 (1989).
[9] M. Richter, M. Meyer, M. Pahler, T. Prescher, E. v. Raven, B. Sonntag, and H. E. Wetzel, Phys. Rev. A **39**, 5666 (1989).
[10] U. Becker, R. Holzel, H. G. Kerkhoff, B. Langer, D. Szostak, and R. Wehlitz, in *Abstracts of Contributed Papers, Fourteenth International Conference on the Physics of Electronic and Atomic Collisions, Palo Alto, CA*, 1985, edited by M. J. Coggiola, D. L. Huestis, and R. P. Saxon (North-Holland, Amsterdam, 1985), p. 12.
[11] A. Mäntykenttä, H. Aksela, S. Aksela, A. Yagishita, and E. Shigemasa, J. Phys. B **25**, 5315 (1992).
[12] A. Mäntykenttä, H. Aksela, S. Aksela, J. Tulkki, and T. Åberg, Phys. Rev. D **47**, 4865 (1993), and references therein.
[13] V. Radojevic, M. Kutzner, and H. P. Kelly, Phys. Rev. A **40**, 727 (1989).
[14] C. W. Clark, J. A. D. Matthew, M. G. Ramsey, and F. P. Netzer, Phys. Rev. A **40**, 4902 (1989).
[15] I. M. Band and M. B. Trzhaskovskaya, J. Electron Spectrosc. Relat. Phenom. **96**, 171 (1998).
[16] T. Matila and H. Aksela, J. Phys. B **33**, 653 (2000).
[17] N. Berrah, B. Langer, A. A. Wills, E. Kukk, J. D. Bozek, A. Farhat, and T. W. Gorczyca, J. Electron Spectrosc. Relat. Phenom. **101-103**, 1 (1999).
[18] H. Aksela, S. Aksela, and H. Pulkkinen, Phys. Rev. A **30**, 865 (1984).
[19] A. N. Nesmeyanov, *Vapour Pressure of the Chemical Elements* (Elsevier, Amsterdam, 1963).
[20] M. Y. Amusia, V. K. Ivanov, and L. V. Chernysheva, Phys. Lett. **59A**, 191 (1976).
[21] R. D. Cowan, *The Theory of Atomic Structure and Spectra* (University of California Press, Berkeley, 1981).
[22] T. Åberg, Phys. Rev. **156**, 35 (1967).
[23] For curve fitting the program SPANCF was used. URL: http://www.geocities.com/ekukk
[24] W. H. Press, S. A. Teukolsky, W. T. Vetterling, and B. P. Flannery, *Numerical Recipes in C* (Cambridge University Press, Cambridge, 1992).
[25] G. B. Armen, B. I. Craig, F. P. Larkins, and J. A. Richards, J. Electron Spectrosc. Relat. Phenom. **51**, 183 (1990).
[26] W. T. Cheng, E. Kukk, D. Cubaynes, J.-C. Chang, G. Snell, J. D. Bozek, F. J. Wuilleumier, and N. Berrah, Phys. Rev. A **62**, 062 509 (2000).
[27] M. Ya. Amusia, in *VUV and Soft X-Ray Photoionization*, edited by U. Becker and D. A. Shirley (Plenum, New York, 1996), p. 1.
[28] M. Ya. Amusia, L. V. Chernysheva, and K. L. Tsemekhman, J. Phys. B **23**, 393 (1990).